Crucial events, randomness, and multifractality in heartbeats

Gyanendra Bohara,[1] David Lambert,[1] Bruce J. West,[2] and Paolo Grigolini[1]
[1]*Center for Nonlinear Science, University of North Texas, P.O. Box 311427, Denton, Texas 76203-1427, USA*
[2]*Information Science Directorate, Army Research Office, Research Triangle Park, North Carolina 27708, USA*
(Received 10 June 2017; published 29 December 2017)

We study the connection between multifractality and crucial events. Multifractality is frequently used as a measure of physiological variability, where crucial events are known to play a fundamental role in the transport of information between complex networks. To establish the connection of interest we focus on the special case of heartbeat time series and on the search for a diagnostic prescription to distinguish healthy from pathologic subjects. Over the past 20 years two apparently different diagnostic techniques have been established: the first is based on the observation that the multifractal spectrum of healthy patients is broader than the multifractal spectrum of pathologic subjects; the second is based on the observation that heartbeat dynamics are a superposition of crucial and uncorrelated Poisson-like events, with pathologic patients hosting uncorrelated Poisson-like events with larger probability than the healthy patients. In this paper, we prove that increasing the percentage of uncorrelated Poisson-like events hosted by heartbeats has the effect of making their multifractal spectrum narrower, thereby establishing that the two different diagnostic techniques are compatible with one another and, at the same time, establishing a dynamic interpretation of multifractal processes that had been previously overlooked.

DOI: 10.1103/PhysRevE.96.062216

I. INTRODUCTION

The hypothesis that multifractality is a significant property of physiological processes gained attention in the literature over the past 20 years. Ivanov *et al.* [1] initiated this interest using wavelets to analyze the heartbeat data of several patients, some healthy and some affected by congestive heart failure. They determined that the main difference between the healthy and nonhealthy is that the healthy subjects have a significantly broader multifractal spectrum. The multifractal approach [1] is an efficient way to measure cardiovascular *variability* [2], referred to as heart rate variability (HRV), the proper treatment of which is still the object of intense discussions [3].

The statistical analysis of heartbeat sequences, as well as that of other physiological processes, is carried out by properly processing suitable time series. Each time series corresponds to a single individual who is unique, thereby raising the challenging problem of determining how to establish a connection with the Gibbs ensemble perspective, which requires averages to be taken over identical copies of the same system. This dilemma is settled by assuming that different portions of the single time series can be interpreted as identical copies of the same process, corresponding to different initial conditions. A well-known analysis technique of this kind is *detrended fluctuation analysis* (DFA) [4,5]. Due, in part, to the growing interest in multifractality [6], Kantelhardt *et al.* [7] extended DFA so as to make it possible to extract from it multifractal information, through the spectral density $f(\alpha)$, which often has the form of a broad inverted parabola that is expected to become very narrow and centered on the scaling index $\alpha = 0.5$ in the ordinary Poisson case. We refer to the algorithm developed in Ref. [7] as multifractal detrended fluctuation analysis (MFDFA). MFDFA is adopted to discuss the transmission of multifractality from a complex network stimulus to another complex network [8], both being characterized by a broad $f(\alpha)$ spectrum.

The main purpose of the present article is to uncover the dynamical origin of a broad $f(\alpha)$ spectrum by moving from the specific case of HRV to the general properties of non-Poisson time series. To achieve this, we follow the search for a diagnostic distinction between healthy and pathological subjects. The goal, however, is to obtain a better understanding of the dynamical origin of multifractal variability. Significant insights about this dynamic origin would attract general interest to the improvement of diagnostic techniques. One possible road to the solution of this problem can be found by noticing that in 2002 Allegrini *et al.* [9] used the detection of crucial events as the main criterion to distinguish healthy [with a broad $f(\alpha)$ spectrum] from unhealthy [with narrow $f(\alpha)$ spectrum] patients. For a proper definition of crucial events we adopt the theoretical perspective established in earlier work, see, for example, Ref. [10], defining the *crucial events* on the basis of the time interval between the occurrence of two consecutive events. The time interval between two consecutive events is described by a waiting time probability density function (PDF) $\psi(\tau)$. In the case of crucial events $\psi(\tau)$ has the asymptotic inverse power-law (IPL) structure:

$$\psi(\tau) \propto \frac{1}{\tau^{\mu}}, \tag{1}$$

with $\mu < 3$. The time intervals between two different pairs of consecutive events are not correlated:

$$\langle \tau_i \tau_j \rangle \propto \delta_{ij}. \tag{2}$$

The occurrence of crucial events plays an important role in the transport of information from one complex network to another [11].

A. Updating the definition of crucial events

It is important to discuss the dynamical origin of events of this kind. Crucial events are a manifestation of cooperative interactions between the units of a complex network that is expected to lead to a spontaneous organization process, usually called self-organized criticality (SOC). Significant progress has been made in understanding SOC since the original work

of Bak *et al.* [12]. The emergence of SOC is signaled by the births of anomalous avalanches; see Refs. [13,14] for recent work along these lines. There exists a new approach to SOC emphasizing temporal rather than intensity anomalous distributions [15,16]. The authors of Ref. [16] defined their approach to self-organization as *self-organized temporal criticality* (SOTC). According to SOTC the crucial events defined earlier with the help of Eqs. (1) and (2), namely the events that the authors of Ref. [9] were able to find in heartbeats, occur on an intermediate time scale, after an initial transient regime to the condition of intermediate asymptotics. The IPL nature of crucial events is tempered by an exponential relaxation in the long-time limit. This interpretation allows us to facilitate our approach to the connection between the diagnostic techniques of Refs. [1] and [9]. In fact, the three time regimes of SOTC are a form of variability that we subsequently connect to the physiological variability that led the authors of Ref. [1] to their diagnostic insight.

In summary, the crucial events are responsible for the complexity of the intermediate asymptotics regime, as it will be more extensively pointed out in Sec. III. Furthermore, we have to take into account that according to Ref. [9] the definition of crucial events must be extended to consider the case where the time interval between the occurrence of the crucial events defined by Eqs. (1) and (2) is filled with events with memory. The first crucial event activates the generation of the filling events and the occurrence of the next crucial time event ends this sequence and activates a new sequence of strongly correlated filling events. The events filling the time interval between two crucial events must not be confused with the Poisson-like events disturbing the healthy physiological function of the heartbeats. In Ref. [9] the events filling the time distance between two consecutive crucial events were responsible for a phenomenon called *memory beyond memory effect*. The intuitive interpretation of this effect is that the crucial events with $\mu < 3$ are responsible for slowly decaying correlation functions, thereby implying a form of memory. The filling events have an additional memory preventing them from disturbing the healthy physiological function signaled by the crucial events. The real heartbeat process is a superposition of two time series, the former corresponding to the healthy function and the later being given by a sequence of totally uncorrelated events.

In this paper the surrogate time sequences are generated adopting for the healthy time series two different prescriptions. The first prescription fits the direction of Ref. [9]. For simplicity's sake, we establish the highly correlated nature of the filling events by making the assumption that time distance τ between two consecutive pseudo events is constant. The distribution of τ is an inverse power law with μ significantly larger than 3, including $\mu = \infty$, namely an ordinary Poisson process. Of course, in this case the crucial renewal condition of Eq. (2) is violated. The later time series, of perturbing Poisson-like events, is generated by deriving the time distance between two consecutive events from a distribution density with $\mu > 3$ identical to that of the filling events of the former. As we shall see, these perturbing Poisson-like events reproduce very well the disturbing process responsible for heart failure. We adopt also the second prescription, where the healthy time series hosts only crucial events and the wide laminar region between two consecutive crucial events is left empty. This simple prescription makes it possible for us to illustrate the efficiency of the method of diffusion entropy analysis (DEA) [17] to determine the scaling generated by the crucial events, but it cannot be used to explain how to establish the percentage of disturbing Poisson-like events. The simple prescription, however, is convenient to show that crucial events alone can generate the multifractal distribution. We shall refer to the first prescription as generating *dressed crucial events* and to the second as generating *bare crucial events*.

B. Outline of the paper

The outline of this paper is as follows. We devote Sec. II to a short review of the earlier attempts at finding a connection between multifractality and crucial events. Section III affords intuitive arguments on the importance of intermediate asymptotics for the analysis of heartbeats illustrated in this paper. Section IV shows why DEA works without being limited to the Gaussian condition. In Sec. V, we show that the use of DEA adopted in earlier work [9] corresponds to the observation of the intermediate asymptotic region. Section VI reviews the procedure adopted in Ref. [9] to process the heartbeat data for the purpose of revealing, with the help of surrogate data, to what extent this is a genuine way of disclosing the contribution of uncorrelated Poisson-like events to the reduction of HRV. Section VII illustrates the joint use of DEA and the evaluation of the percentage of uncorrelated Poisson-like events. Finally, Sec. VIII is devoted to concluding remarks.

II. SCALING AND MULTIFRACTALITY

The search for crucial events is made difficult by the fact that crucial events are often imbedded in clouds of uncorrelated and irrelevant events. The authors of Ref. [9] used a technique of statistical analysis, called DEA [17], to detect the anomalous scaling index δ, which these crucial events would generate were they not imbedded in a cloud of noncrucial events, namely, when they are visible. However, to establish a connection with the results of Ivanov *et al.* [1] it is necessary to address a problem that goes beyond the merely diagnostic goal of both Refs. [1] and [9]. The problem is to uncover the physical mechanism producing the multifractality revealed by MFDFA. This problem has been the subject of many research papers and we devote this Section to a short review of the results of that research.

A key element of this debate is the DEA, which was shown to be the correct way to determine the scaling generated by crucial events while DFA is not [18–20]. This is a consequence of the fact that DFA determines the scaling of the second moment of a distribution that can be divergent for non-Gaussian distribution densities. For this reason many attempts have been made to combine the correct scaling evaluation with the evaluation of multifractality [19–24]. However, these interesting papers leave unanswered the central question of the multifractal significance of crucial events, since these authors applied the new technique of analysis to real data with no discussion of surrogate data hosting only crucial events.

It is convenient, for the sake of clarity, to mention some papers from the field of experimental psychology [25–28].

For our purposes, the merit of these publications is that they establish, through their analysis of real data, a connection between multifractality and the transport of information. In this way they imply a connection between multifractality and the crucial events revealed by the proper use of DEA, in accordance with the observation that crucial events play an important role in the transport of information from one complex network to another [11].

Finally, it is important to mention that Refs. [29] and [30] examine a nonstationary human network by means of DEA that enables them to reveal the existence of periodicity and complexity simultaneously. Sarkar and Barat [30] adopt DEA to examine heartbeats before and after meditation, with the surprising discovery of a distinct oscillatory behavior of diffusion entropy. We shall come back to discuss the results of Ref. [30] in Sec. VIII. Here we limit ourselves to properly addressing the connection between crucial events and multifractality by adopting surrogate sequences with a mixture of Poisson-like and crucial events, including the case where only crucial events are hosted in the sequence. Such surrogate sequences enable us to assess how crucial events are perceived by MFDFA. This is the case where it is useful to use the prescription for bare crucial events.

According to the statistical analysis of Ref. [9] the distinction between healthy and pathologic subjects is established by noting that the heartbeat dynamics of pathologic subjects host a critically large number of uncorrelated Poisson-like events. An important result of this paper is the observation that uncorrelated Poisson-like events have the effect of reducing HRV. The largest HRV is realized in the ideal case of cardiac dynamics uniquely determined by the SOTC process, with its complete time evolution including the transient regime, intermediate asymptotics with its crucial events of Eqs. (1) and (2), and the final tempered asymptotic regime. The dressed crucial events are a form of randomness signaling the healthy physiological function of heartbeats, while the uncorrelated Poisson-like events represent a disturbance of this healthy physiological function and for this reason we refer to them either as randomness or strong randomness, when they reach the high concentration revealed by our analysis in the case of heart failure. In addition to results of diagnostic interest, this paper starts down the road to a deeper understanding of the dynamical origin of multifractality.

III. INTERMEDIATE ASYMPTOTICS

In his book on intermediate asymptotics [31], Barenblatt adopts a visual art metaphor to illustrate the concept of intermediate asymptotics: "We have to look at paintings at a distance great enough not to see the brush-strokes, but at the same time small enough to enjoy not only the painting as a whole but also its important details: think of van Gogh's work, for example...." Goldenfeld [32] illustrates the renormalization group rules that we have to adopt to eliminate the divergences created by the perturbation approach. This illustration is based on the assumption that the physical condition of intermediate asymptotics is a form of perennial transition to equilibrium.

There is a wide conviction that this is a simplifying but useful idealization of reality. A remarkable example is afforded by the work of Mantegna and Stanley [33]. These authors noticed that although a finite size-induced truncation is an unavoidable consequence of the dynamics of real physical processes, the time duration of the transition to the Gaussian statistics prescribed by the central limit theorem may become extremely extended, in line with the idealized condition of perennial intermediate asymptotics of Goldenfeld. However, for practical purposes a complex system can also be observed on so large a time scale as to see dynamical effects that for simplicity may be interpreted as forms of ordinary fluctuation-dissipation processes. Important work has been done to obtain analytical results for both short- and long-time regimes; see, for instance, Ref. [34], which triggered significant interest in the appropriate mathematical formalism of transient anomalous diffusion [35], including the exponential form of tempering [36,37]. It is convenient to notice that tempering may be an effect of representing real physical processes by means of finite length time series, an unavoidable consequence of observation. We believe [16] that tempering is a genuine property of the process of self-organization itself, since it emerges from the interaction of a finite number of units and that the heartbeat process belongs to this class of self-organizing processes, thereby involving tempering.

IV. DIFFUSION ENTROPY

DEA makes it possible to evaluate the correct scaling of a diffusion process, regardless of whether the Gauss condition applies or not [17]. The scaling index δ of a diffusing variable x is defined by

$$p(x,t) = \frac{1}{t^{\delta}} F\left(\frac{x}{t^{\delta}}\right), \tag{3}$$

where $p(x,t)$ is the PDF of the variable x at time t and $F(y)$ is a function that for crucial events does not have the ordinary Gaussian form. DEA measures the Shannon entropy of the diffusion process:

$$S(t) = -\int_{-\infty}^{+\infty} dx p(x,t) \ln[p(x,t)]. \tag{4}$$

By substituting Eq. (3) into Eq. (4), after some algebra and replacing the integration variable x with the integration variable $y = x/t^{\delta}$, we obtain [17]

$$S(t) = A + \delta \ln(t), \tag{5}$$

where the constant reference entropy is

$$A \equiv -\int_{-\infty}^{+\infty} dy F(y) \ln[F(y)]. \tag{6}$$

Equation (5) shows that the entropy $S(t)$ increases linearly with $\ln(t)$ and the slope of the resulting straight line is the scaling coefficient δ. The numerical search for the scaling coefficient is done with this property in mind. Changing the unit adopted to measure time changes the value of t, but does not affect the scaling parameter δ [17]. DFA is based on evaluating scaling through the second moment of $p(x,t)$ and this has the effect of providing misleading information on δ when $p(x,t)$ has an IPL tail so slow as to generate divergence. For this reason, Yazawa in his recent work on the effects of emotions on HRV adopted a modified version of DFA [38]. However, the MFDFA used herein is based on the adoption

of fractional moments $\langle |x|^q \rangle$, thereby bypassing the problems created by slow diffusion IPL tails with a conveniently small value of q.

V. DEA AS A TECHNIQUE TO REVEAL CRUCIAL EVENTS

The DEA method [17] was originally introduced to properly analyze time series assumed to be driven by crucial renewal events. It is important to stress that the renewal events hypothesized [9] for the analysis of heartbeats are the subject of an extended literature focusing on the phenomenon of renewal aging [39]. For a friendly illustration of the main results of this paper, we remind the readers about an algorithm used to generate non-Poisson renewal events. It is given by [11,40]

$$\tau = T\left(\frac{1}{y^{\frac{1}{\mu-1}}} - 1\right), \tag{7}$$

where y is a real number selected with uniform probability on the interval $(0,1)$. The times τ generated by this algorithm are totally uncorrelated and obey the waiting time PDF

$$\psi(\tau) = (\mu-1)\frac{T^{\mu-1}}{(\tau+T)^{\mu}}. \tag{8}$$

Note that to be as close as possible to the tempering prescriptions of SOTC [16], we should adopt a survival probability $\Psi(t)$ with the structure

$$\Psi(t) = \left(\frac{T}{t+T}\right)^{\mu-1} \exp(-\lambda t), \tag{9}$$

with the transient regime to intermediate asymptotics being determined by the parameter T and defined by the time region $0 < t < T$. The time region of intermediate asymptotics corresponds to $T < t < \frac{1}{\lambda}$ and the tempered region is given by $t > \frac{1}{\lambda}$. For simplicity's sake the surrogate sequences hereby used are established using Eq. (7), which would correspond to $\lambda \to 0$, the tempered action being exerted by the finite size of the time series, L. We make the assumption that $\lambda \propto 1/L$.

In this paper, following the results of earlier work [9], we limit our analysis to the IPL index range:

$$2 < \mu < 3. \tag{10}$$

It is important to stress that the Poisson events correspond to $\mu = \infty$, but events drawn from $\mu = 5$ are sufficiently far from the crucial condition to be used as generators of noncrucial events. The algorithm of Eq. (7) can be used to explain in an intuitive way the different nature of the randomness of $\mu < 3$ as compared to that of $\mu \gg 3$. The time interval between two consecutive choices of the random number y in Eq. (7) has the mean value

$$\langle \tau \rangle = \frac{T}{(\mu-2)}, \tag{11}$$

as can be easily established using the waiting time PDF $\psi(t)$ of Eq. (8) to perform the average. If $\langle \tau \rangle < \Delta t$, where Δt is the integration time step, we observe a process that is totally random. In the limiting case of $\mu < 2$, $\langle \tau \rangle \gg \Delta t$, since in this case $\langle \tau \rangle$ is divergent; the randomness is sporadic. In the region $2 < \mu < 3$ randomness is not as sporadic as for $\mu < 2$. However, $\langle \tau^2 \rangle$ is divergent and as a consequence randomness remains distinctly intermittent. We make the assumption that the sporadic randomness of crucial events is good for the healthy function of cardiac dynamics and that an excess of randomness is risky.

To discuss the joint action of frequent and sporadic randomness let us create suitable surrogate time series, namely an appropriate sequence of times $\tau_1, \tau_2, \ldots . \tau_i, \tau_{i+1}, \ldots .$ This sequence is generated by a repeated random selection of y in Eq. (7) so as to create either a sequence of crucial events, with $\mu < 3$, or a sequence of noncrucial events, with $\mu > 3$. More precisely, in the applications of the present paper we adopt $3 > \mu > 2$ for crucial events and $\mu = 5$ for noncrucial events.

Each of these two time sequences has to be turned into a corresponding suitable fluctuation $\xi(t)$. To do that we adopt the Asymmetric Jump Model (AJM) [9]. The reason for this choice is that this random walk rule makes it possible for DEA to reveal the correct scaling established by the generalized central limit theorem (GCLT) [41] in the whole crucial event region $\mu < 3$, including the region $\mu < 2$. This random walk rule is established by setting $\xi = 0$ when there are no events, and $\xi = 1$ when either a crucial or uncorrelated Poisson event occurs.

Thus we create two time series, one corresponding to $\mu < 3$ and one corresponding to $\mu > 3$. The surrogate time series used here for the statistical analysis corresponds to the superposition of both time series,

$$\xi(t) = (1 - \in)\xi_{\mu>3}(t) + \in \xi_{\mu<3}(t). \tag{12}$$

The parameter $\in < 1$ is the probability that the observed heartbeat signal, detected according to the prescription of the next section is generated by a genuine SOTC process. The prescription adopted to generate the complex time series is the prescription earlier mentioned as generating bare crucial events. In Sec. VI we explain how to derive $\in$ from the analysis of real heartbeat data, with the help of surrogate time series when we adopt the prescription to generate dressed crucial events.

In the case where SOTC events are visible, namely $\in = 1$, the method of DEA leads to the detection of the proper scaling,

$$\delta = \frac{1}{\mu-1}, \tag{13}$$

after an initial transient corresponding to the microtime regime, where the complexity of the process is not yet perceived. Notice that the transition from the Lévy to the Gauss regime occurs at $\mu = 3$. However, as stated earlier, the surrogate time series of this paper rest on $\mu = 5$, namely a condition well imbedded in the Gaussian basin of attraction.

Figures 1–3 show the results of applying DEA to a variety of data sets through the linear-log representation, which is used, according to Sec. IV, to detect the scaling δ, the slope of the linear portion of $S(t)$ in this representation.

Figure 1 illustrates the case where $\in = 1$, namely the condition where the bare crucial events are fully visible, with $\mu = 2.2$. The corresponding crucial scaling should be $\delta = 0.83$. However, in the short time regime the scaling has the larger value $\delta = 1.5$ and the scaling $\delta = 0.83$ of crucial events appears in the intermediate time regime. For this reason, the proper scaling, as shown in this figure, is optimal in the

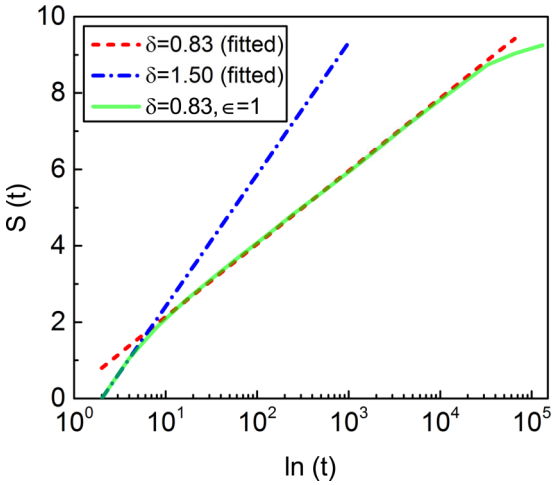

FIG. 1. Entropy of the time series versus the logarithm of time from the microtime to the asymptotic time scale with $\in = 1$. The solid line (green) is numerical. Numerical constants are $T = 0.5$ and length of time series $L = 1.5(10^5)$. We use the prescription generating bare crucial events.

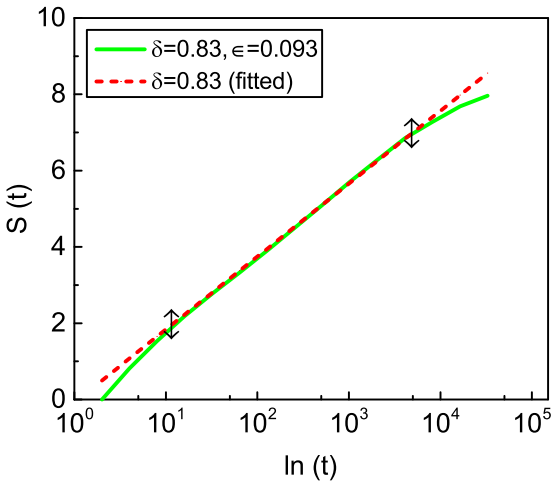

FIG. 3. DEA detects the scaling of invisible crucial events in the intermediate asymptotic time. The solid line (green) is obtained from real heartbeat data of healthy individual. The scaling δ is the slope of the straight line between the two vertical arrows.

intermediate time regime. Actually, we see that in the region around $t \propto 10^5$ a tempering deviation from the crucial scaling of Eq. (13) occurs. Note that this is not the tempering of the SOTC defined in Ref. [16]. The theoretical study of that physical tempering of the process is outside the scope of the present paper, but we make the plausible assumption that heartbeat dynamics fit it as a consequence of being itself a self-organized process.

Figure 2 illustrates the more important case where the crucial events are hidden by a cloud of noncrucial events. In this case, too, according to earlier analysis [9], the correct scaling generated by the bare crucial events appears in the intermediate time regime. However, in this case the reason for the initial transient is quite different from the SOTC initial transient. In this case, the initial short-time regime characterized by the conventional scaling $\delta = 0.5$ corresponds to the scaling of uncorrelated Poisson-like events. In the long-time regime, when the SOTC intermediate asymptotic emerges, the faster scaling of the crucial events with $\mu < 2$ leads them to crossover to ordinary diffusion. The overlap of the Poisson-induced transient regime and transient SOTC make the derivative of the diffusion entropy nonmonotonic. For simplicity's sake we do not show this complicated behavior, instead we focus on the complexity of the intermediate asymptotics. Notice that, although the extended transient to the intermediate asymptotic regime induced by a large percentage of uncorrelated Poisson-like events can be confused with the transient SOTC regime, the corresponding physical effects are the opposite of one another. The SOTC transient generates a broad multifractal spectrum, while the long transient induced by a large percentage of uncorrelated Poisson-like events has the effect of making the multifractal spectrum narrower.

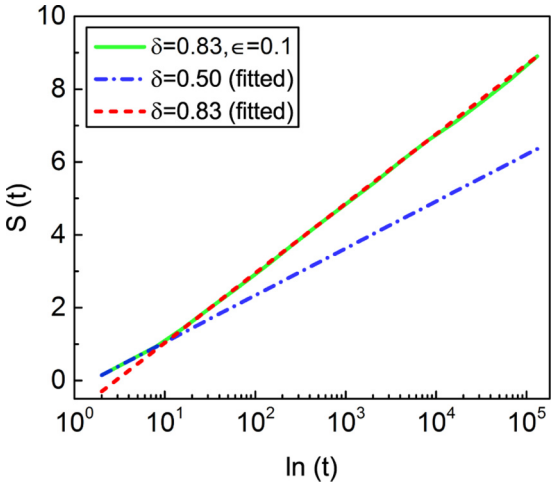

FIG. 2. Entropy of the time series versus the logarithm of time from the microtime Gaussian basin of attraction to the asymptotic time scale with $\in = 0.1$. The solid line (green) is numerical. Numerical constants are $T = 0.5$ and length of time series $L = 1.5(10^5)$. We use the prescription generating bare crucial events.

To complete the discussion of this section we make some comments concerning Fig. 3. In Sec. VI we explain how to derive this figure from real data on heartbeats. Here we limit our observation to the scaling index δ, representing the indicator of the occurrence of crucial events. The IPL index is evaluated by monitoring the intermediate asymptotics region, the short- and long-time limit of which are denoted by vertical arrows. In this case, the deviation from Eq. (13) of the tempering region is probably due the properties of heartbeats, rather than to the finite-size L of the sequence under study.

In summary, it is important to reiterate that on the basis of recent advances made concerning SOTC [16], the time series generated by complex processes are characterized by three regimes: the short-time regime, where the true complexity of the process is not yet perceived; an intermediate-time regime driven by the crucial events; and a long-time regime where the process can be mistaken for an ordinary statistical process. The long-time regime is, on the contrary, a tempering effect generated by self-organization.

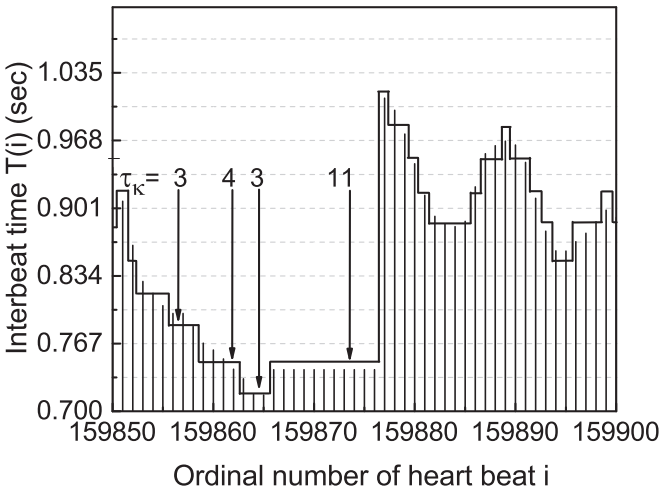

FIG. 4. Rule adopted to define events. An event is defined as the experimental curve, thick black line, crossing the border between two consecutive strips. The symbols τ_k indicate the time distance, in terms of number of beats, between two consecutive events, defined as the black line crossing from one strip to one of the neighbor strips. The size of the strips is $\Delta T = 1/30$ s.

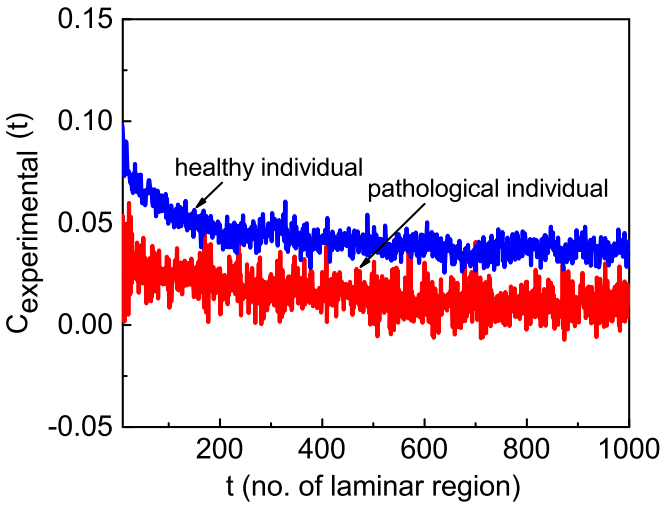

FIG. 5. Correlation function $C(t)$ for two typical patients, one healthy and one pathological.

VI. HOW TO PROCESS EXPERIMENTAL DATA TO REVEAL THE EXISTENCE OF CRUCIAL EVENTS

Following Refs. [42] and [9], we use the ECG records of the MIT-BIH Normal Sinus Rhythm Database and of the BIDMC Congestive Heart Failure Database, for healthy and congestive heart failure patients, respectively.

The main problems encountered in proving that SOTC is the process driving the phenomenon under study has to do with the detection of the crucial events, namely, events with a waiting time PDF yielding a diverging second moment. Figure 4 shows the approach we adopt, following that used earlier in Ref. [9]. The experimental signal is obtained by assigning to each beat a value corresponding to the time interval between one and the next.

We divide the interbeat time axis into small strips of size ΔT. We follow the results of the analysis done in Ref. [43] to define ΔT. These authors suggest $\Delta T \cong 30$ ms and we set $\Delta T = 33$ ms. We define the occurrence of an event as the experimental signal crossing from one strip to one of the two nearest neighbor strips. We see that the heartbeat trajectory may remain in a given strip for an extended time, suggesting the typical intermittent behavior that led to the discovery of crucial events. However, the experimental signal crossing the border between two contiguous strips is not necessarily a crucial event. The crucial events are renewal and consequently the times τ_i should not be correlated. To assess the breakdown of the renewal condition we evaluate the time-average correlation function, where the time average is indicated by an overbar:

$$C(t) = \frac{\sum_{|i-j|=t} \overline{(\tau_i - \overline{\tau})(\tau_j - \overline{\tau})}}{\sum_i \overline{(\tau_i - \overline{\tau})^2}}. \tag{14}$$

This correlation function is properly normalized, thereby yielding $C(0) = 1$, and in the case of genuine renewal events should satisfy the condition $C(t) = 0$ for $t > 0$. On the contrary we find

$$C(1) \approx \epsilon^{\,2}, \tag{15}$$

where ϵ is the probability of selecting ξ; see Eq. (12). This result is theoretically explained by noticing that according to Ref. [43] the correlation function $C(t)$ should read

$$C(t) = (1 - \epsilon^2)\delta_{t,0} + \epsilon^2\, \Lambda(t), \tag{16}$$

where $\delta_{t,0}$ denotes the Kronecker unit step function, namely a function equal to 1 for $t = 0$ and equal to 0 otherwise, and $\Lambda(t)$ is a slowly decaying smooth function with the property $\Lambda(0) = 1$. This theoretical prediction yields Eq. (15).

In summary, we should use $C(1)$ to define ϵ. The analysis of real data as depicted in Fig. 5 leads to conclusions that qualitatively agree with this theoretical prediction, with some warming, however. Figure 5 shows that the correlation function $C(t)$ makes an abrupt jump from 1 to a very small, but nonvanishing value of ϵ^2, confirming that the analysis we adopt to reveal events actually does not detect only genuine renewal events, but a mixture of renewal and nonrenewal events. Furthermore, as shown from Fig. 5, in the case of pathological individuals, $C(t)$, after the fall undergoes fast intense fluctuations that may prevent us from defining ϵ^2 through $C(1)$. In this case, and in the case where $C(1) < 0$ as well, we alternatively define $C(1)$ through the mean value over the first 100 events. In the case of fluctuations of moderate intensity, we use $C(1)$ to define ϵ^2. We also use Fig. 5 to define the border between strong and weak randomness. Values of ϵ^2 larger than 0.05, $\epsilon > 0.22$, are referred to as weak randomness and values of ϵ^2 smaller than 0.05, $\epsilon < 0.22$, are referred to as strong randomness. This definition is suggested by the observation of the healthy and pathological individual of Fig. 5, but this definition must be used with caution because the distinction between healthy and pathological individuals, as shall see with Fig. 8, requires the knowledge of the scaling index δ as well as that of ϵ^2.

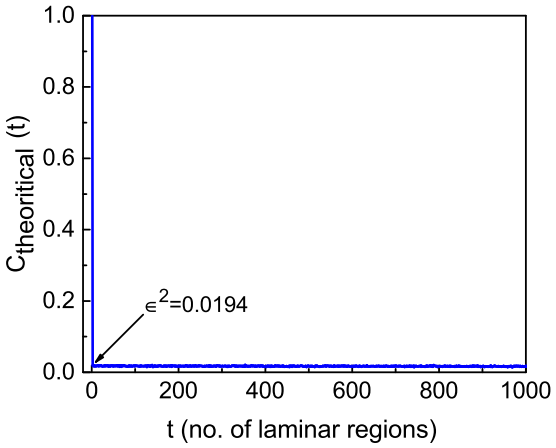

FIG. 6. Correlation function C(t) for the surrogate data in the case of strong randomness. We use the prescription generating dressed crucial events.

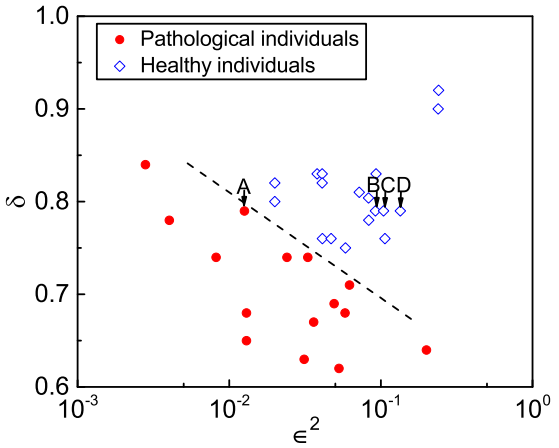

FIG. 8. Distinguishing subjects with healthy from those with pathological HRV.

To get a better understanding of the meaning of ϵ^2, and to explain the theoretical reason why we can use Eq. (15), we interrogate the surrogate sequences defined by Eq. (12), in the case when the sequel of crucial events is created by the prescription to generate dressed crucial events. With the help of Figs. 6 and 7, we establish that the intensity ϵ^2 is the square of the probability that an event is a crucial event. This is the reason why we adopt the symbol ϵ^2 to denote the value of the correlation C(t) immediately after the abrupt jump down from $C(0) = 1$. Figure 6 shows a theoretical correlation function using a surrogate sequence for strong randomness. Figure 7 shows a theoretical correlation function using a surrogate sequence for weak randomness.

It is worth stressing that the choice of $\Delta T = 1/30$ s is not arbitrary. In fact, investigators [43] establish that the value of ΔT leads to the maximal value of ϵ^2 for all patients, both healthy and pathological patients, except for the transplanted hearts. This universal property seems to imply the action of the autonomic system [43].

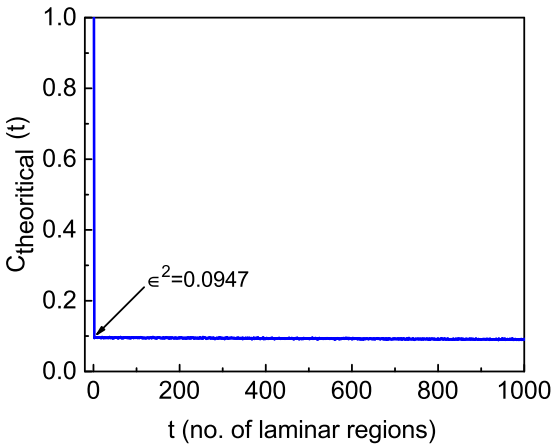

FIG. 7. Correlation function $C(t)$ for the surrogate data in the case of weak randomness. We use the prescription generating dressed crucial events.

VII. JOINT USE OF DEA AND C(t)

In this section, we recover the central result of Ref. [9], which was based on the joint use of DEA and the correlation function $C(t)$. For each subject we calculate both δ and ϵ^2.

In fact, Fig. 8 is virtually identical to the central result found by the authors of Ref. [9], which establishes a criterion to distinguish pathological patients from healthy patients using HRV time series. We notice that the ideally healthy condition corresponds to $\epsilon = 1$ and $\delta = 1$. This means that the crucial events should not host any uncorrelated Poisson-like event and should have $\mu = 2$, which is the border between the region of perennial aging, $\mu < 2$, and the region where the rate of randomness production becomes constant in the long-time limit, $\mu > 2$ [11]. The patients' HRVs move toward the pathological condition as their scaling becomes closer to the scaling of ordinary diffusion $\delta = 0.5$, namely closer to the border between the region of crucial events, $\mu < 3$, and the Gaussian basin of attraction, $\mu > 3$.

Note that the work of Ref. [10] established that the brain, generating ideal $1/f$-noise, is located at the border between the region of perennial aging and the region of crucial events hosted by heartbeats, according to the analysis of this paper and earlier work [9].

The research work done in the new field of network medicine [44] focuses on the interaction between the different organs of the human body, the brain and heart being a special case of this intercommunication [45]. According to the *principle* of *complexity matching* [11], based on the assumption that the synchronization of complex networks is facilitated by the networks sharing the same complexity, $\mu = 2$, in the case of brain-heart communication, we make the plausible conjecture that the right-top corner of Fig. 8 corresponds to a convenient condition for brain-heart communication in the ideal case of healthy patients. However, the current literature on complexity matching emphasizes the communication between the two complex networks through their multifractal spectra [8]. Therefore, establishing a connection between crucial events and multifractal spectra is a goal of this paper. The most important property of Fig. 8 is to contribute to the realization

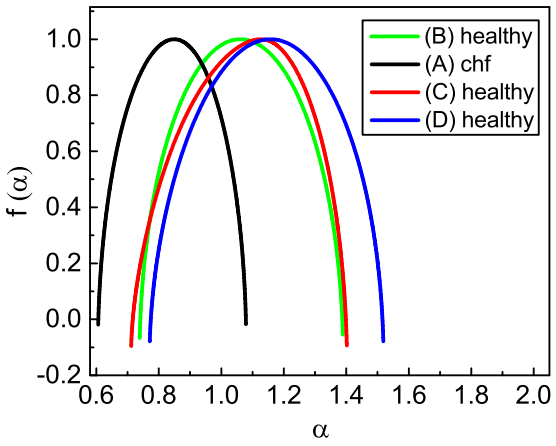

FIG. 9. Multifractal spectra of HRV as a function of $\in$ (see Fig. 8) keeping constant the crucial scaling $\delta = 0.79$.

of that goal by establishing a connection between Refs. [9] and [1,42].

We focus our attention on the individuals labeled A, B, C, and D in Fig. 8. These patients have the same δ and according to the earlier analysis [9] the distinction between sick and healthy patients is due to the fact that the heartbeat of the sick patients is affected by excessive randomness. Furthermore, according to some investigators [1,42] the distinction is due to the fact that healthy patients have broader multifractal spectra.

The central result of the present paper is obtained by applying the MFDFA to the individuals A, B, C, and D for the purpose of proving the connection between the diagnostic recipe of Ref. [9] and that of Refs. [1,42].

Figure 9 fully confirms this connection. We see, in fact, that moving from the sick (A) to the healthy patients (B,C,D) has the effect of increasing the width of the multifractal spectrum. Note that Fig. 10 provides additional confirmation of this connection through the use of surrogate sequences.

VIII. CONCLUDING REMARKS

The diagnostic method generated by following earlier work [9] yields additional benefits compared to the technique of

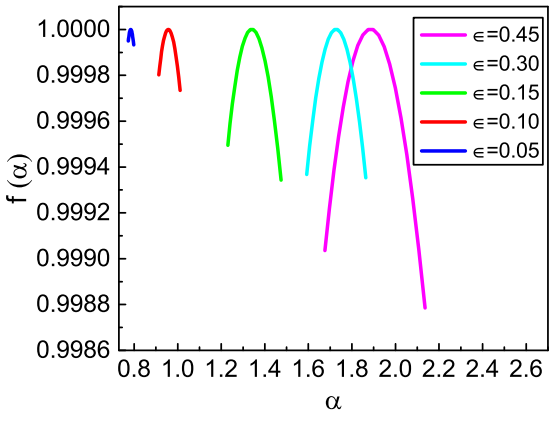

FIG. 10. Multifractal spectra of surrogate data, based on the prescription generating bare crucial events, as a function of $\in$ keeping constant the crucial scaling $\delta = 0.83$.

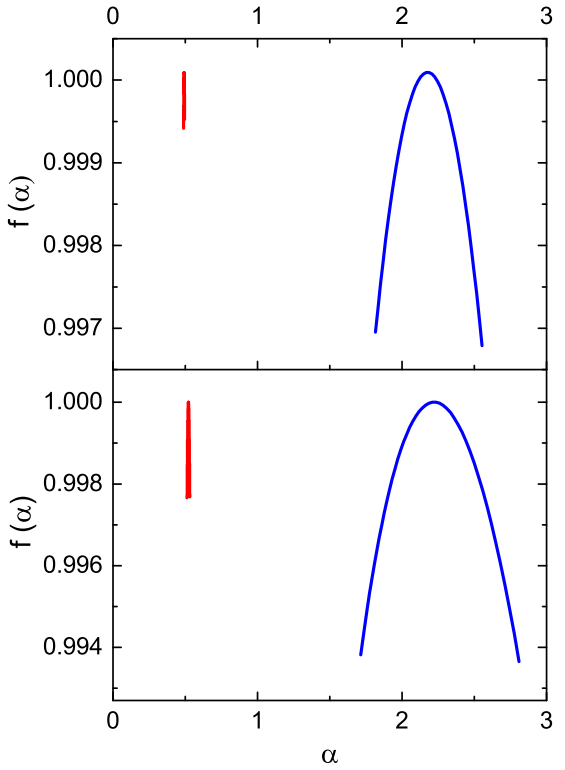

FIG. 11. Extreme cases of most narrow, $\in = 0$, and most broad, $\in = 1$, multifractal spectra. The top panel is based on the prescription generating bare crucial events and the bottom panel is based on the prescription generating dressed crucial events. Numerical constants used in the calculation are $T = 0.5$, $L = 1.5(10^5)$, window sizes $(500 : 500 : 30000)$. Other parameters are moments range $q = -0.4 : 0.001 : 0.4$ for $\mu = 2.2$ and $q = -0.02 : 0.001 : 0.02$ for $\mu = 5$.

Ref. [1]. One of these benefits is that the distinction between healthy and pathologic patients is established through the two-dimensional representation of Fig. 8 rather than the three-dimensional representation of Ref. [1]. Another important result of the present paper is its contribution to an improved vision of variability and multifractality. To appreciate this significant improvement let us focus our attention on the results obtained by applying the MFDFA to the surrogate series in the limiting case of a SOTC [16] process, unperturbed by uncorrelated Poisson-like fluctuations $\in = 1$, and of a mere sequence of uncorrelated fluctuations, $\in = 0$.

The result of this analysis is shown in Fig. 11. In the top panel of this figure we adopt the prescription to generate bare crucial events and in the bottom we adopt the prescription to generate dressed crucial events. Of course, in the case $\in = 0$ both prescriptions generate a very sharp multifractal distribution centered on $\alpha = 0.5$.

The narrowest multifractal spectrum is realized by setting $\in = 0$. The broadest multifractal spectrum is realized in the absence of Poisson-like random events, $\in = 1$, with a slight difference between mere crucial events(top panel of Fig. 11) and dressed crucial events (bottom panel of Fig. 11). The dressed crucial events are shown to yield a broader multifractal spectrum.

We reiterate that, according to SOTC [16], crucial events are characterized by three distinct time regimes, a transient

initial regime, the intermediate asymptotics time regime, and a final tempered time regime with exponential truncation. The transient time regime becomes more and more extended with decreasing $\in$. However, the extended transient regime generated by a very small value of $\in$ must not be confused with a wide transient regime corresponding to the occurrence of a sufficient number of crucial events to realize the prescription $\delta = 1/(\mu - 1)$ of the GCLT [17,41]. The GCLT transient regime is the micro-evolution towards the IPL regime predicted by SOTC [16]. This transient regime, the intermediate asymptotic time regime and the final tempering time regime are the generators of the wide variability that the multifractal DFA efficiently detects. The uncorrelated Poisson-like events with $\mu > 3$ generate an extended transient regime that has the opposite effect of yielding an extremely narrow spectrum around the ordinary scaling value $\alpha = 0.5$.

In conclusion, the results of the present paper establish a connection between the multifractal spectrum and SOTC fluctuations, thereby affording a promising tool to make further progress in the field of network medicine [44], where broad multifractal spectra are transferred, according to Ref. [11], from one network to another via crucial events.

The research program laid out in this paper is not complete, since we have not, as yet, addressed the brain-heart communication and the influence of periodicity [45]. It is important to notice that SOTC [16] can be used to produce a self-organization phenomenon combining crucial events and periodicity, so as to convert the black line of Fig. 4 into fluctuations that under the influence of either therapeutic action [46] or meditation [30] may become almost coherent oscillations. In the recent literature there are conflicting statements about the analysis of the same data, under the influence of meditation, leading some authors [47] to claim that the $f(\alpha)$ spectrum broadens and the others [48] to claim that it becomes narrower. We believe that these oscillations, even if distinctly coherent, host crucial events and that the transport of information from one coherentlike network to another, for instance, the α waves of the brain and the heartbeats, depends on crucial events, with μ slightly larger than 2, for both networks [9,10]. Meditation favors coherence [30] and the brain-heart communication if the unhealthy randomness of uncorrelated Poisson-like events is kept under control. The research work of Correll [49] showed that addressing difficult tasks has the effect of turning the time series generated by the brain, which would yield $1/f$ noise, into a generator of white noise, thereby implying the increase of the probability of uncorrelated Poisson-like events. This leads us to the conjecture to test with future research work that stress has the effect of increasing the concentration of uncorrelated Poisson-like events thereby contributing to the incidents of heart failure. On the other hand meditation [30] and therapeutic action [46] may have the opposite effect of reducing the unhealthy randomness of uncorrelated Poisson-like events and of increasing the healthy randomness of SOTC crucial events.

ACKNOWLEDGMENTS

The authors thank Welch and ARO for financial support through Grants No. B-1577 and No. W911NF-15-1-0245, respectively.

[1] P. C. Ivanov, L. A. N. Amaral, A. L. Goldberger, S. Havlin, M. G. Rosenblum, Z. R. Struzikk, and H. E. Stanley, Multifractality in human heartbeat dynamics, Nature **399**, 461 (1999).

[2] T. Force, Heart rate variability: Standards of measurement, physiological interpretation, and clinical use, Eur. Hearth J. **17**, 354 (1996).

[3] A. Bravi, A. Longtin, and A. JE. Seely, Review and classification of variability analysis techniques with clinical applications, Biomed. Eng. **10**, 90 (2011).

[4] C.-K. Peng, S. V. Buldyrev, S. Havlin, M. Simons, H. E. Stanley, and A. L. Goldberger, Mosaic organization of DNA nucleotides, Phys. Rev. E **49**, 1685 (1994).

[5] S. M. Ossadnik, S. B. Buldyrev, A. L. Goldberger, S. Havlin, R. N. Mantegna, C.-K. Peng, M. Simons, and H. E. Stanley, Correlation approach to identify coding regions in DNA sequences, Biophys. J. **67**, 64 (1994).

[6] G. Paladin and A. Vulpiani, Anomalous scaling laws in multifractal objects, Phys. Rep. **156**, 147 (1987).

[7] J. W. Kantelhardt, S. A. Zschiegner, E. Koscielny-Bunde, S. Havlin, A. Bunde, and H. E. Stanley, Multifractal detrended fluctuation analysis of nonstationary time series, Physica A (Amsterdam) **316**, 87 (2002).

[8] D. Delignieres, Z. M. H. Almurad, C. Roume, and V. Marmelat, Multifractal signatures of complexity matching, Exp. Brain Res. **234**, 2773 (2016).

[9] P. Allegrini, P. Grigolini, P. Hamilton, L. Palatella, and G. Raffaelli, Memory beyond memory in heart beating, a sign of a healthy physiological condition, Phys. Rev. E **65**, 041926 (2002).

[10] P. Allegrini, D. Menicucci, R. Bedini, L. Fronzoni, A. Gemignani, P. Grigolini, B. J. West, and P. Paradisi, Spontaneous brain activity as a source of ideal $1/f$ noise, Phys. Rev. E **80**, 061914 (2009).

[11] B. J. West, E. L. Geneston, and P. Grigolini, Maximizing information exchange between complex networks, Phys. Rep. **468**, 1 (2008).

[12] P. Bak, C. Tang, and K. Wiesenfeld, Self-Organized Criticality: An Explanation of *1/f* Noise, Phys. Rev. Lett. **59**, 381 (1987).

[13] S. Zapperi, K. B. Lauritsen, and H. E. Stanley, Self-Organized Branching Processes: Mean-Field Theory for Avalanches, Phys. Rev. Lett. **75**, 4071 (1995).

[14] M. Martinello, J. Hidalgo, S. di Santo, A. Maritan, D. Plenz, and M. A. Muñoz, Neutral theory and scale-free neural dynamics, arXiv:1703.05079.

[15] E. Lipiello, L. De Arcangelis, and C. Godano, Memory in self-organized criticality, Europhys. Lett. **72**, 678 (2005).

[16] K. Mahmoodi, B. J. West, and P. Grigolini, Self-organizing complex networks: Individual versus global rules, Front. Physiol. **8**, 478 (2017).

[17] N. Scafetta and P. Grigolini, Scaling detection in time series: Diffusion entropy analysis, Phys. Rev. E **66**, 036130 (2002).

[18] C. Shi-Min, P. Hu, Y. Hui-Je, Z. Tao, Z. Pei-Ling, and W. Bing-Hong, Scaling behaviour and memory in heart rate of healthy human, Chin. Phys. Lett. **24**, 3002 (2007).

[19] P. Jizba and J. Korbel, Multifractal diffusion entropy analysis: Optimal bin width of probability histograms, Physica A (Amsterdam) **413**, 438 (2014).
[20] J. Huang, P. Shang, and X. Zhao, Multifractal diffusion entropy analysis on stock volatility in financial markets, Physica A (Amsterdam) **391**, 5739 (2012).
[21] A. Y. Morozov, Comment on multifractal diffusion entropy analysis on stock volatility in financial markets, Physica A **392**, 2442 (2013).
[22] H. Yang, F. Zhao, L. Qi, and B. Hu, Temporal series analysis approach to spectra of complex networks, Phys. Rev. E **69**, 066104 (2004).
[23] Y. Yujun, L. Jianping, and Y. Yimei, Multiscale multifractal multiproperty analysis of financial time series based on Rényi entropy, Int. J. Mod. Phys. C **28**, 1750028 (2017).
[24] J. Huang and P. Shang, Multiscale multifractal diffusion entropy analysis of financial time series, Physica A (Amsterdam) **420**, 221 (2015).
[25] D. Mirman, J. R. Irwin, and D. G. Stephen, Eye movement dynamics and cognitive self-organization in typical and atypical development, Cogn. Neurodynam. **6**, 61 (2012).
[26] J. A. Dixon, J. H. Holden, D. Mirman, and D. G. Stephen, Multifractal dynamics in the emergence of cognitive structure, Topics Cognitive Science **4**, 51 (2012).
[27] D. G. Kelty-Stephen, K. Palatinus, E. Saltzman, and J. A. Dixon, A tutorial on multifractality, cascades, and interactivity for empirical time series in ecological science, Ecol. Psychol. **25**, 1 (2013).
[28] D. G. Stephen and A. Hajnal, Transfer of calibration between hand and foot: Functional equivalence and fractal fluctuations, Atten. Percept. Psychophys **73**, 1302 (2011).
[29] S. Scellato, M. Musolesi, C. Mascolo, and V. Latora, On Nonstationarity of Human Contact Networks, in *Proceedings of the International Conference on Distributed Computing Systems* (2010), pp. 105–111.
[30] A. Sarkar and P. Barat, Effect of meditation on scaling behavior and complexity of human heart rate variability, Fractals **16**, 199 (2008).
[31] G. I. Barenblatt, *Scaling, Self-similarity, and Intermediate Asymptotics* (Cambridge University Press, Cambridge, 1996).
[32] N. Goldenfeld, *Lectures on Phase Transitions and the Renormalization Group* (Addison-Wesley Publishing Company, Reading, MA, 1992).
[33] R. N. Mantegna and H. E. Stanley, Stochastic Process with Ultraslow Convergence to Gaussian: The Truncated Lévy Flight, Phys. Rev. Lett. **73**, 2946 (1994).
[34] I. Koponen, Analytic approach to the problem of convergence of truncated Levy flights towards the Gaussian stochastic process, Phys. Rev. E **52**, 1197 (1995).
[35] A. Chakrabarty and M. M. Meerschaert, Tempered stable laws as random walk limits, Stat. Prob. Lett. **81**, 989 (2011).
[36] M. M. Meerschaert, P. Roy, and Q. Shao, Parameter estimation for exponentially tempered power law distributions, Commun. Stat. Theory Methods **41**, 1839 (2012).
[37] R. Uppu and S. Mujumdar, Exponentially Tempered Lvy Sums in Random Lasers, Phys. Rev. Lett. **114**, 183903 (2015).
[38] T. Yazawa, Invisible emotion, anxiety and fear: Quantifying the mind using EKG with mdfa, systemics, Cybernet. Informat. **15**, 1690 (2017).
[39] S. Burov, R. Metzler, and E. Barkai, Aging and nonergodicity beyond the Khinchin theorem, Proc. Natl. Acad. Sci. USA **107**, 13228 (2010).
[40] Eq. (7) is Eq. (180) of Ref. [11] with $(\mu - 1)$, misprint, correctly replaced by $1/(\mu - 1)$.
[41] W. Feller, Trans. Am. Math. Soc. **67**, 98 (1949).
[42] A. L. Goldberger, L. A. N. Amaral, L. Glass, J. M. Hausdorff, P. C. Ivanov, R. G. Mark, J. E. Mietus, G. B. Moody, C.-K. Peng, and H. E. Stanley, PhysioBank, PhysioToolkit, and PhysioNet, Circulation **101**, e215 (2000).
[43] P. Allegrini, R. Balocchi, S. Chillemi, P. Grigolini, L. Palatella, and G. Raffaelli, *Short- and Long-Term Statistical Properties of Heartbeat Time-Series in Healthy and Pathological Subjects*, in *Medical Data Analysis, Third International Symposium, Lecture Notes in Computer Science*, edited by G. Goos, J. Hartmanis, and J. van Leeuwen (Springer, Berlin, 2002), p. 115.
[44] P. C. Ivanov, K. K. L. Liu, and R. P. Bartsch, Focus on the emerging new fields of network physiology and network medicine, New J. Phys. **18**, 100201 (2016).
[45] G. Pfurtscheller, A. R. Schwerdtfeger, A. Seither-Preisler, C. Brunner, C. S. Aigner, J. Brito, M. P. Carmo, and A. Andrade, Brain-heart communication: Evidence for "central pacemaker" oscillations with a dominant frequency at 0.1 Hz in the cingulum, Clin. Neurophysiol. **128**, 183 (2017).
[46] R. McCraty and M. A. Zayas, Cardiac coherence, self-regulation, autonomic stability, and psychological well-being, Front. Psycho. **5**, 1090 (2014).
[47] A. Bhaduri and D. Ghosh, Quantitative assessment of heart rate dynamics during meditation: An ECG based study with multifractality and visibility graph, Front. Physiol. **7**, 44 (2016).
[48] R. Song, C. Bian, and Q. DY. Ma, Multifractal analysis of heartbeat dynamics during meditation training, Physica A (Amsterdam) **392**, 1858 (2013).
[49] J. Correll, *1/f* noise and effort on implicit measures of bias, J. Pers. Soc. Psychol. **94**, 48 (2008).